# A Review of Photonic Systems-on-Chip Enabled by Widely Tunable Lasers

Larry A. Coldren, *Life Fellow, IEEE*, Paul A. Verrinder, and Jonathan Klamkin, *Senior Member, IEEE*

*Abstract*—**Photonic Integrated Circuits (PICs) on indium phosphide have matured significantly over the past couple of decades and have found use in many system applications. Some PIC efforts on other group III-V substrates have also been initiated. In numerous cases, the usefulness of these PICs is because of the reduction in size, weight, and power they provide, but in many cases also because of the higher performance made possible by the improved relative phase stability among optical paths as well as the reduction of inter-element coupling losses. In this paper, as part of this special issue in tribute to Prof. Daniel Dapkus, we focus on monolithic PICs that provide a system function, especially those that incorporate and build on widely-tunable laser technology as a key element. Some of the early widely-tunable laser work is reviewed, and a selection of past system-on-a-chip developments is presented as background. Then, more recent system-on-a-chip advances performed by the author's groups are reviewed in more detail. Key advances are highlighted.**

*Index Terms*—**Optoelectronics, photonics, photonic-integrated-circuits, semiconductor lasers, tunable lasers.**

## I. Introduction

**T**HIS paper reviews recent research at the University of California Santa Barbara (UCSB) on relatively complex photonic integrated circuits (PICs) based on III-V materials that perform a useful optical system function. These PICs, denoted as System-on-Chip (SoC)-PICs [1], are generally closely packaged, or co-packaged, with control or complementary functional electronics. Similar work has also been carried out at other academic and industrial laboratories, and some of this work has been summarized in prior reviews [1]–[10].

The focus of this paper is on monolithic SoC-PICs on native III-V substrates, including both indium phosphide (InP) and gallium arsenide (GaAs), which incorporate tunable lasers as a key component. It is, however, worth noting that considerable work has also been carried out in recent years in the area of hybrid and heterogeneous integration of III-V materials on silicon. Approaches include, co-packaging, wafer

bonding, micro-transfer printing, as well as direct growth of III-V materials on silicon [11]–[14]. These technologies were developed primarily for datacom applications [15], [16].

The UCSB work has especially highlighted the benefit of using widely-tunable lasers as an integral part of most of their SoC-PICs. As will be discussed in Section II below, past examples of these SoC-PICs have included: optical transmitters, receivers, all-optical switches, coherent receivers, vector transmitters, and LIDAR transceivers. Incorporation of widely-tunable lasers has provided full C-band operation, and in the case of LIDAR, wide beam sweep angles. The background in Section II will begin with some discussion of the origins of widely-tunable lasers.

In Section III, our recent work will show improved coherent receivers with lower power dissipation and noise, better SoC-PICs for RF-over-fiber transmission, very rapid switching and phase locking for agile frequency synthesis, high-power optical transmitters for free-space links, a SoC-PIC and electronics for gas absorption sensing using frequency-swept LIDAR, and the demonstration of a widely-tunable laser PIC on gallium arsenide for the 1 $\mu$m wavelength region.

## II. Background

### A. Early PICs on III-Vs

A history of III-V PICs has been recently reported by Kish, *et al.* in [1]. As outlined therein, the concept and promise of PICs was first suggested by Miller in 1969 [17]. Low-loss fiber in the 1300-1550 nm wavelength range soon followed in the early 1970s [18] leading to intensive research on quaternary indium gallium arsenide phosphide (InGaAsP) and related materials on InP that have bandgap wavelengths in this range. By the late-1970s many of the desired active and passive components—lasers, lasers with gratings, passive waveguide couplers, modulators, detectors, etc.—had been demonstrated [1].

Early in the 1980s, fiber optic links had been introduced at 1300 nm, but even at the modest data rates used then, links were limited in reach to 30-40 km by the available signal-to-noise ratio. Expensive electronic repeaters were required to regenerate the signals at that point. To avoid this optical-electrical-optical (OEO) conversion, research on coherent technologies was initiated to extend the reach to approximately 80 km by leveraging the increased sensitivity afforded by coherent detection. A relatively coarse wavelength division multiplexing (WDM) was also being employed, and coherent could assist with the demultiplexing. Coherent and WDM
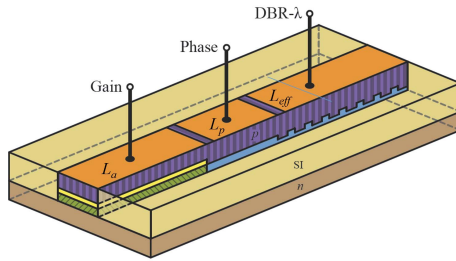
Fig. 1.    Three-section tunable laser with one DBR and one cleaved facet mirror. Phase and DBR sections are passive (no gain), but tunable with current. The gain section provides gain with current injection, but little tuning. For more information see [21], [22].
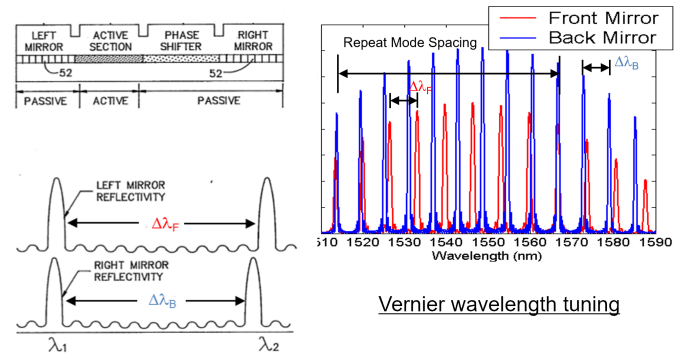


Fig. 2.    Four-section widely-tunable laser. (Left) Excerpts from USP #4,896,325 illustrating basic structure and Vernier concept; (right) simulated mirror reflection spectra, expanding to many mirror reflection peaks, and showing eventual repeated overlaps.

stimulated some device researchers to begin work on tunable lasers, which could serve both as universal sources for WDM transmitters and tunable local oscillator (LO) sources that could be phase locked to the incoming signal in a coherent receiver [19], [20].

Researchers at the Tokyo Institute of Technology led by Prof. Suematsu were some of the first to focus on 1550 nm because optical fiber should ultimately have the lowest loss at this wavelength. They also realized that lasers should be tunable to operate as a WDM or coherent source, and they should have grating mirrors to be integrable with other passive waveguides and devices. They demonstrated such devices in the early 1980s [3].

By the late 1980s, relatively mature three-section DBR tunable lasers had been developed by several companies and universities [21], [22]. As shown in Fig. 1, these consisted of an active gain section, a passive phase tuner, and a passive Distributed-Bragg-Reflector (DBR) mirror, all connected to separate electrical sources. The active gain section contains gain material with a bandgap near the lasing wavelength in its *pn* junction, and the passive sections have higher bandgap material in their *pn* junctions, which change their index of refraction when current is injected. With current injected into the DBR, the narrow band over which it reflects is shifted in wavelength in proportion to the index shift. The optical cavity modes do not shift as much, so current must also be applied to the phase section to shift the cavity modes. In practice, approximately 6-7 nm of wavelength shift is possible at 1550 nm.

By the late 1980s coherent had still not been widely adopted. Higher data rates, denser WDM, as well as simply using more parallel fibers had been satisfying the increased demand, which was still due to a somewhat slowly increasing demand for voice, not data; the disruptive data crossover was not to occur until around 2000. By the late 1980s, research on the erbium-doped fiber amplifier (EDFA) was also beginning to show promise [23]. With the EDFA, OEO repeaters were no longer necessary and new links designed for the mid-1990s and beyond would no longer use OEO repeaters only for signal regeneration for modest distances. Work on coherent subsequently slowed.

### B. Widely-Tunable Lasers

The EDFA enabled WDM over approximately 40 nm of bandwidth at 1550 nm in what was to be called the center or C-band. So, those researchers working on tunable lasers immediately began to search for concepts to make widely-tunable lasers, ones that could encompass the entire C-band.

There were a few ideas already being considered. For example, some of the early tunable laser work used coupled cavities, and these made use of Vernier tuning between the cavity modes of the two different length cavities to select a single mode [24]. However, these never led to a widely-tunable result, generally because the cavity modes were too close together. A relatively simple solution came in 1988 with the invention of the four-section tunable laser with two 'differing multi-element mirrors' [25], as described in Fig. 2.

By using periodically blanked, periodically modulated, or 'sampled' gratings, the reflection spectra of the gratings, instead of being a single sharp peak, are broken into a number of image peaks forming reflection combs. This is the so-called Sampled-Grating DBR, or SGDBR. If the two gratings are sampled with a different period, the period of the two reflection combs are different, but the separation of the reflection peaks can be large (~6-7 nm), and the separation difference can be tailorable (~1 nm). Thus, there is only one net reflection maximum for the laser (product of the two mirrors), and the repeat between these can be ~40 nm for single mode operation. By shifting both mirrors together, and then shifting one relative to the other slightly to select another pair of mirror maxima, and again repeating the shift together, it is possible to cover the full 40 nm with a single net maximum without missing any wavelengths [26].

Figure 3 shows the first results with the SGDBR laser in 1992 [27]. Although it did not include a phase tuner for fine tuning, it did illustrate the potential of the design with a total discontinuous tuning range of 57 nm and good single mode behavior over most of that range. Besides showing the fundamental attributes of the design, it should be noted that the material was grown by Prof. Dapkus' group, illustrating one additional element of his influence on our field. Also, on this subject, we should mention that most of the early work at UCSB was supported by metalorganic chemical vapor deposition (MOCVD) growths performed by the group of Prof. DenBaars, an alumnus of Prof. Dapkus' research group.
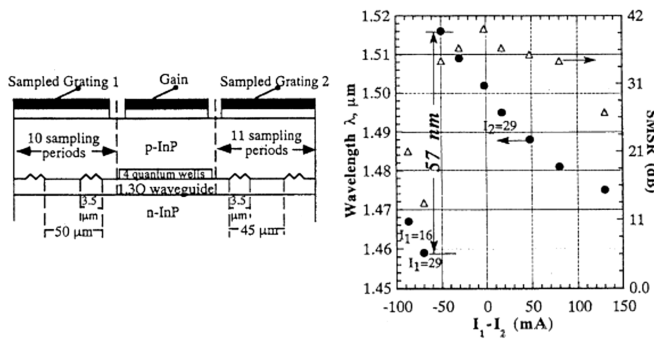
Fig. 3. First demonstration of wide range discontinuous tuning by a SGDBR laser. Adapted with permission from [27].
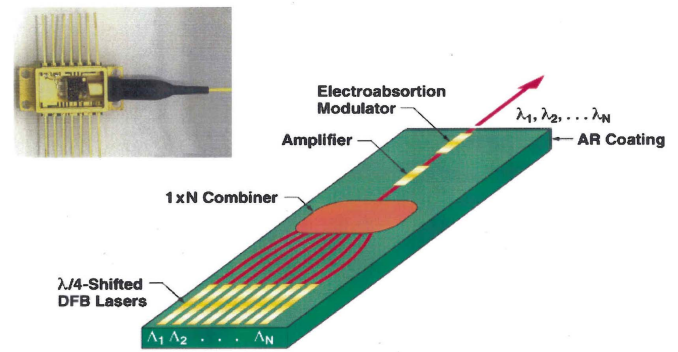


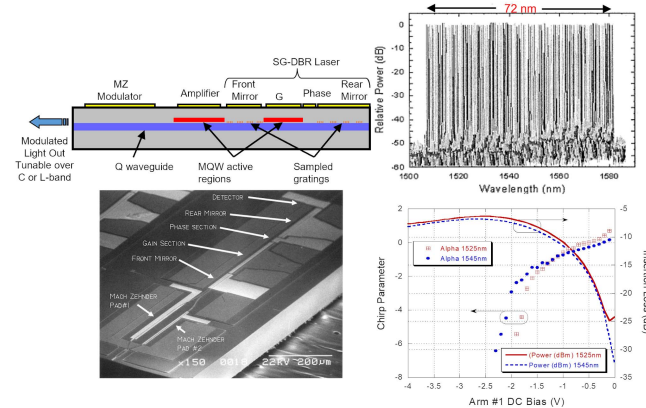Fig. 5. DFB selectable-array PIC. Adapted with permission from [38].



Fig. 4. SGDBR integrated with SOA and MZM schematic together with tuning results, a photograph, and modulator chirp vs. DC bias. For more information see [23] and [24].

The SGDBR design was to become one of the most successful of the options for widely-tunable lasers [28], perhaps the principal reason being that it was no more complex to manufacture than the three-section DBR illustrated in Fig. 1. The additional challenge was in the tuning control, and even that was only marginally more difficult. Following UCSB research, a company was formed, Agility Communications, to develop the concept into a product in 1998. This company also productized more complex PICs that incorporated SGDBRs with monitoring photodetectors, semiconductor optical amplifiers (SOAs), and modulators, either of the electroabsorption (EAM) [29] or Mach-Zehnder (MZM) [30] type.

Figure 4 shows the first UCSB prototype of the SGDBR-SOA-MZM along with chirp results reported in 2002 [23]. Also shown is a wavelength tuning spectrum of 72 nm from an earlier publication in 2000 [24], [25]. The output power at this tuning width was compromised to be ∼1 mW, so practical devices were later designed for ∼40 nm of tuning, which then allowed 40 mW in fiber reported by Agility in 2003 [31].

Agility was acquired by a more established optical components company in 2005, and many millions of these devices were sold into optical systems products that are still in use [32]. Analogous designs using 'differing multi-element mirrors' also appeared by other companies in the early 2000s,

and following some patent litigation, they were licensed to produce products [33].

Another early example stemmed from work on directional couplers between different waveguides. It was known that waveguides with slightly different effective indexes could be coupled if a coarse grating was added to one of them to provide the difference in propagation constants, or the phase matching. But, since this grating is fixed, and the waveguide propagation constants are proportional to frequency, phase matching is satisfied only over a limited bandwidth. However, this band can be tuned over a relatively large range by changing the index of one of the waveguides slightly; this is so because the difference between the waveguide indexes is small, and it is the *ratio* of the index change in one guide to this *difference* between the two waveguide indexes that counts. This concept was investigated by several research groups in the 1990s [34], [35], and eventually a company, Altitune, developed it into a product. However, following an acquisition, the acquiring company decided to abandon the concept.

There were a number of other examples of widely-tunable laser concepts developed in the late 1990s to early 2000s [36], mainly in response to the 'telecom bubble' that resulted from the realization that the rapidly increasing data bandwidth demand curve was overtaking the slowly increasing voice curve. But as dense WDM systems at higher data rates became available, this demand appeared to be satisfied, at least for a few years—perhaps just long enough to burst the bubble [37]. In any event, a couple of the widely-tunable solutions survived and that seemed to be sufficient.

Another concept not mentioned above, but very compelling to many at this time, was a DFB 'selectable-array' PIC, illustrated in Fig. 5. It typically consisted of 8-12 DFB lasers of slightly different wavelength that covered most of the C-band, and these could be tuned thermally by a few nanometers to fill in the gaps [38], [39]. These were all coupled by an MMI coupler into a single waveguide that incorporated an SOA, to compensate the 1/N coupling loss, as well as a possible integrated modulator.

This design was especially popular in Japan, because it seems many companies there were somewhat skeptical about the reliability and stability of the widely-tunable types discussed above [39]. Although the DFB selectable-array is not technically a widely-tunable laser, it does provide the same
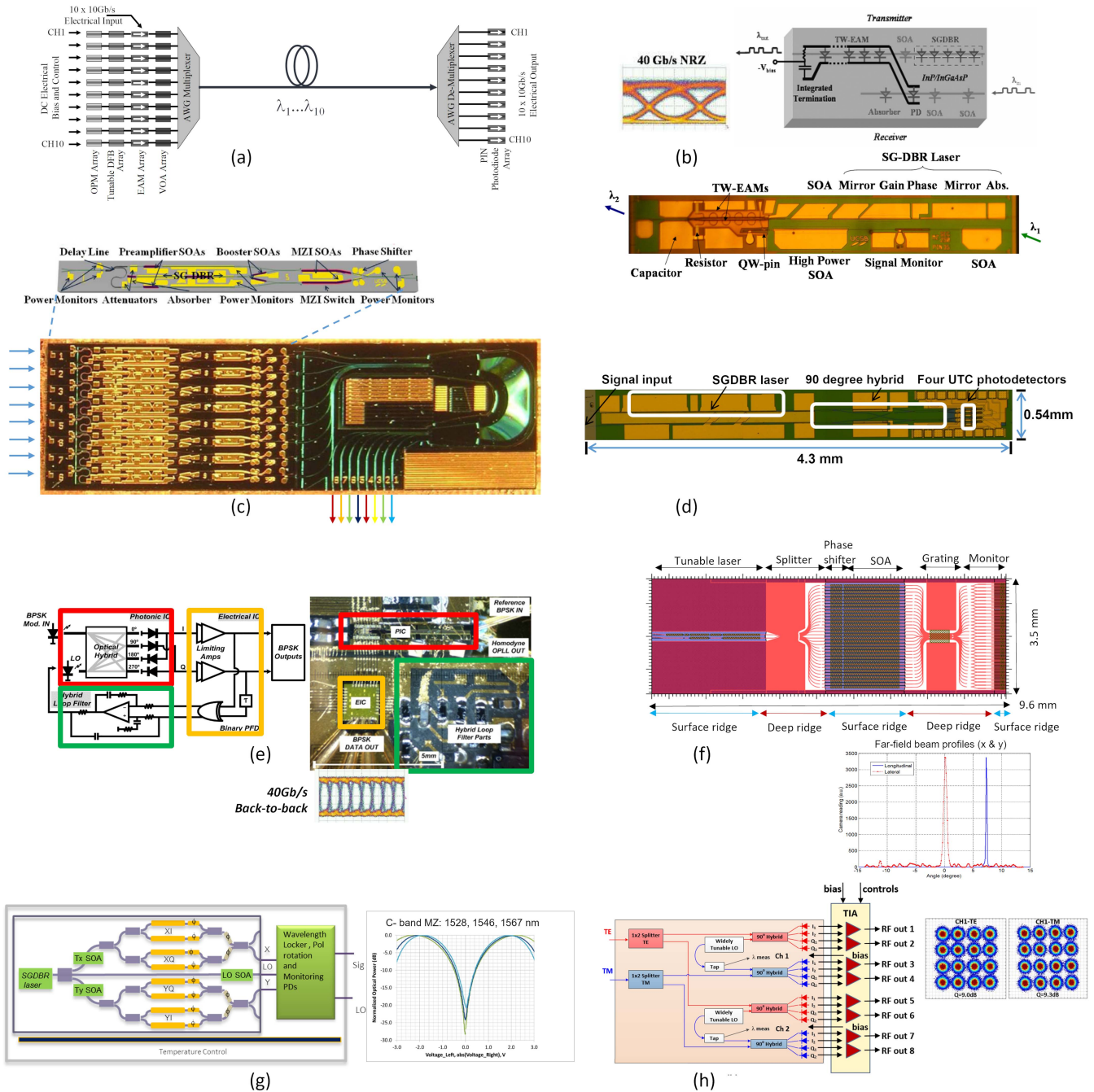
Fig. 6. Sampling of SoC-PIC results from 2004 to 2017. (a) Schematics of $10 \times 10$ Gb/s DFB/EAM integrated with AWG-MUX transmitter PIC and AWG-De-MUX integrated with 10 PIN PD array receiver PIC. Courtesy: Infinera; for more information see [43]; (b) full C-band wavelength-converter/transceiver PIC—SOA-PD input stage and SGDBR-Traveling-wave EAM output stage. Adapted with permission from [44]; (c) $8 \times 8$ all-optical packet switch PIC with 8 non-linear MZM wavelength converters integrated with an $8 \times 8$ AWGR. Adapted with permission from [45]; (d) coherent receiver PIC with high-power, widely-tunable SGDBR-LO, SOA, hybrid, and 4-high-bandwidth PDs. Adapted with permission from [46]; (e) Costa's loop phase-locked C-band coherent receiver. Adapted with permission from [47]; (f) 2-D LIDAR PIC with $32 \times 120$ resolution from 32 surface-emitting waveguides and tunable laser. Adapted with permission from [48]; (g) C-band vector transmitter PIC with supplemental LO output. Courtesy: Lumentum; for more information see [6]; (h) 2-Channel Rx PIC and TIA architecture and recovered constellations at 16 QAM for both polarizations @88 Gbaud. Courtesy: Infinera; for more information see [49].

functionality. Other 'selectable-array' types were also explored during the early 2000s [40]–[42].

### III. SYSTEM-ON-CHIP DEMONSTRATIONS (2004-2017)

Figure 6 shows a sampling of SoC-PIC examples from the period 2004-2017.

The examples of Fig. 6 illustrate that SoC-PICs have provided many different functionalities and that significant savings in size, weight, and power have been demonstrated by integration. For example, as discussed in [1], the transmitter PIC in Fig. 6(a) comprises 10 transmitter channels that each include an optical power monitor, a DFB laser of a

unique wavelength, an EAM, and a variable optical attenuator (VOA) (or SOA), all combined by an arrayed-waveguide grating (AWG) multiplexer. This is co-packaged with a 10-channel analog application specific integrated circuit (ASIC) modulator driver chip and a single thermoelectric cooler (TEC). The co-packaging with a single driver chip and a single TEC enables considerable power savings. A comparable description is provided for the receiver chip in [1], [43].

The discussion is somewhat similar for most of the SoC-PICs in Fig. 6. That is, many photonic elements are combined on a single PIC, the drive or control electronics are co-packaged, and a single TEC is used for the entire PIC. Figure 6(b) shows a data format and rate transparent wavelength converter/regenerator, which only requires DC bias connections, although data monitoring is available [39]. Operation from 5-40 Gb/s was demonstrated, and conversion from any input C-band wavelength to any output C-band wavelength was also confirmed. This SoC-PIC operates somewhat as a transceiver by using the input signal photocurrent from the receiving photodiode to dynamically change the bias on an EAM that follows an on-chip SGDBR laser. A regeneration function is possible by overdriving the EAM. Similar PICs have been constructed with MZMs [50].

Figure 6(c) shows the so-called MOTOR chip [45], which provides all-optical switching between its eight inputs and eight outputs. It operates in the return-to-zero (RZ) format at 40 Gb/s if nonlinear MZI-SOA wavelength converters are used [51]. This restriction is removed if the transceiver type of wavelength converter shown in Fig. 6(b) is employed. The outputs of the wavelength converters are coupled to an arrayed-waveguide-grating-router (AWGR), which sorts them according to their new wavelength to one of the outputs.

Figure 6(d) is a widely-tunable coherent receiver PIC. It includes SOA pre-amplifiers for the incoming signals, an integrated SGDBR-SOA as a high-power LO, a 90-degree hybrid and four uni-traveling-carrier (UTC)-photodiodes, which typically have bandwidths >30 GHz and good power handling capabilities, so that signal plus LO inputs well above the shot-noise level can be used. This receiver can be used with a number of different types of electronics, but it was used primarily in 'analog' coherent receivers in our work. For example, in Fig. 6(e), it is shown in the red box, and we have constructed a Costas phase/frequency locking circuit to phase-lock the LO to the carrier of the incoming signal with a wide frequency capture range [46], [47].

Figure 6(f) illustrates a 2-D optical beam-scanner chip that can be used in LIDAR or other direction-specific illumination or communication applications. The output of an SGDBR-SOA is split into 32 separate waveguides and coupled to an optical phased array via 32 phase shifters and SOAs. Light then emits from a weighted-grating surface-emitter region [48]. The angle of emission in the axial direction is varied by the wavelength. The angle in the lateral direction is varied by adjusting the individual phase shifters of the phased array using a particle-swarm optimization [52]. On-chip monitor photodiodes following the emitter array verify the calibration [52].
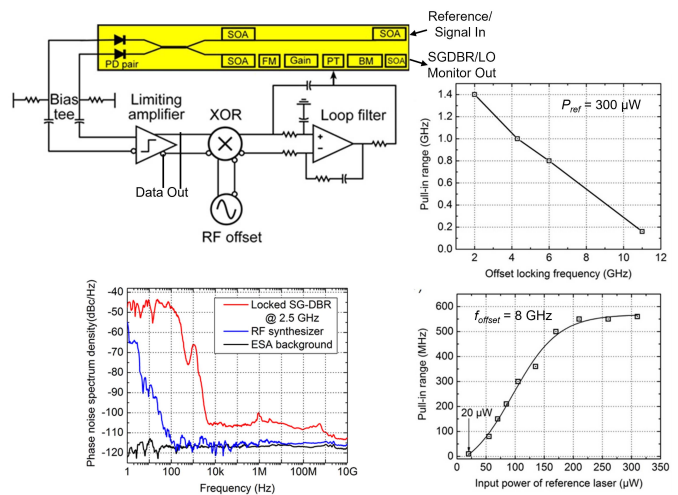


Fig. 7. Heterodyne optical phase locked loop with improved sensitivity and power consumption; schematic, locking frequency pull-in range vs. RF offset and input power of reference, and phase noise spectral density. Adapted with permission from [55].

Figure 6(g) is a schematic of a dual-polarization C-band vector transmitter PIC along with MZM characteristics from Lumentum [6]. This was co-packaged with modulator electronics and a TEC, and it was made available for system vendors. An LO output was also provided for use in a combined transmitter/receiver coherent module [6].

Figure 6(h) is a PIC receiver with transimpedance amplifier (TIA) architecture from Infinera, which uses a $1 \times 2$ splitter at the PIC input. This is capable of up to 720 Gb/s of input at 88 Gbaud over modest distances [49]. In [1], an analogous architecture is described in which the PIC employs a $1 \times 6$ splitter at its input to increase the practical data rate to 1.2 Tb/s at 33 Gbaud over considerably longer distances.

## IV. RECENT SYSTEM-ON-CHIP DEMONSTRATIONS

In the last five years there has been considerable activity at UCSB on SoC-PICs based on III-V materials grown at UCSB. The first section describes examples related to the use of optical phase lock loops (OPLLs) that are improvements on seminal work carried out a few years earlier [53], [54]. The following sections describe high power InP PICs for free space optical communications, InP PICs for remote sensing LIDAR, and tunable laser PICs for 1030 nm applications including topographical LIDAR.

### A. Recent Optical Phase-Locked Loop Experiments

Figure 7 summarizes a more recent heterodyne OPLL effort with improved overall performance characteristics, and with significantly improved input optical sensitivity levels and power dissipation. The theoretical sensitivity was approximately 9 $\mu$W, and 20 $\mu$W was measured with a slight (2.5 GHz) offset [55].

The total dissipated power in the electronics was reduced dramatically to 1.12 W relative to circuits like those from Fig. 6(e), which consumed ~3 W. The power consumption
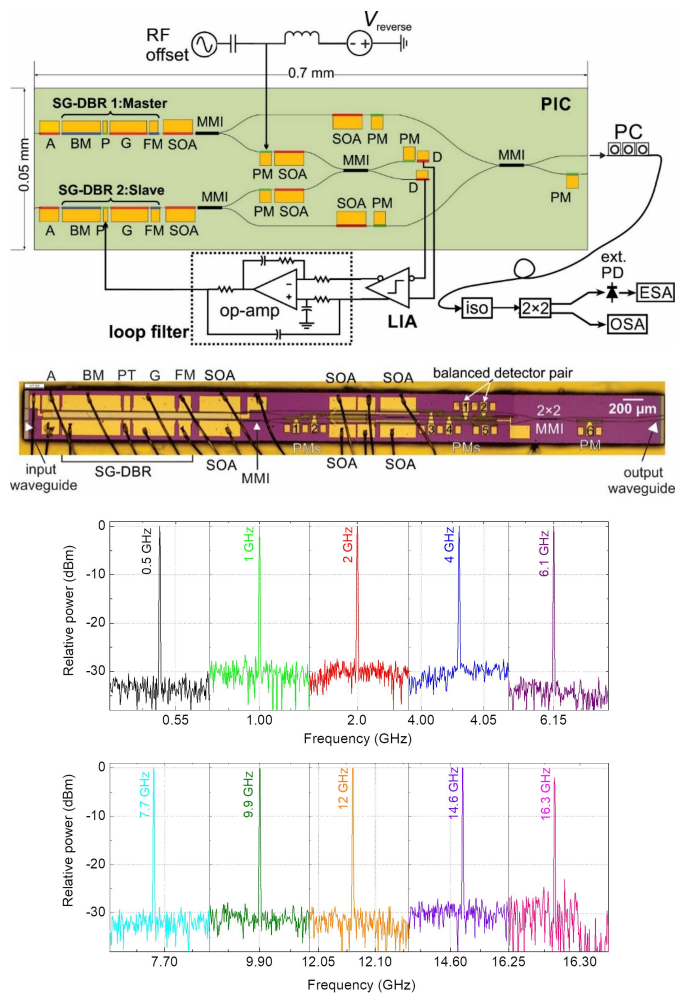
Fig. 8. RF-over-fiber SoC-PIC using an on-chip optical modulator for side-band generation. A schematic (top), PIC photo (center) and ESA spectra for various laser offsets due to RF applied to integrated phase modulator (PM) in center. Adapted with permission from [56].
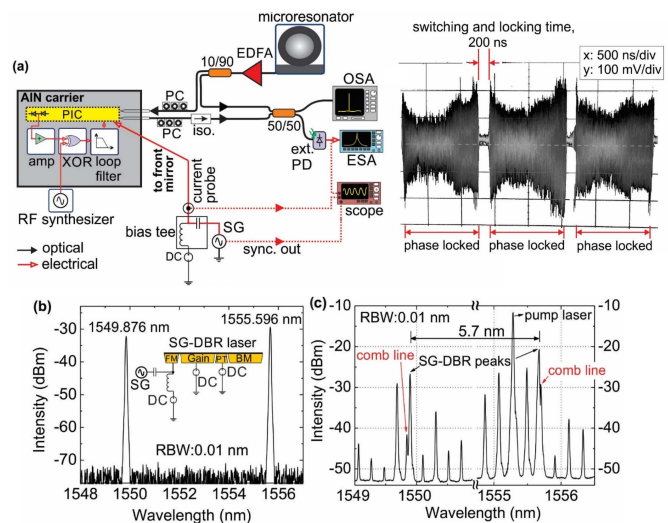
Fig. 9. Rapid locking of on-chip SGDBR laser to external microresonator for stable frequency synthesis. Schematic at top left. RF synthesizer set to 2.5 GHz; 800 kHz square wave applied to SGDBR front mirror to switch wavelength by 5.72 nm. ESA shows switching and locking time (top right); OSA shows spectra at bottom without and with microresonator reference. Adapted with permission from [57].

of the PIC with an SGDBR laser and SOA was 0.66 W with 10 mW output power. Experiments were also carried out with a Y-branch laser-PIC from Freedom Photonics; this PIC consumed only 0.18 W with 10 mW out, the difference being mostly that no SOA was employed [55].

As also illustrated in Fig. 7, the pull-in range of this simple OPLL is limited relative to the Costas-loop design of Fig. 6(e), which has a frequency locking and phase locking capability, because of the I and Q availability. In the case of Fig. 6(e) the pull-in range was ∼20 GHz [46], but here it is limited to ∼1 GHz, dependent in both cases on the signal strength and heterodyne offset.

Figure 8 shows results of an OPLL used to offset lock one SGDBR laser from another in an RF-over-fiber PIC [56]. This OPLL uses the sidebands from an on-chip optical modulator to lock the slave laser to the master rather than an electronic mixer, such as the XOR in Fig. 7. As illustrated by the electrical spectrum analyzer (ESA) spectra, master-slave offset locking up to 16.3 GHz was demonstrated.

In addition to the inner waveguide branches dedicated to the OPLL, this SoC-PIC also has outer waveguide branches

that can be separately modulated to add signals to these two offset-locked laser carrier frequencies. They are combined near the output so that both carriers and possible modulation(s) are summed for transmission [56]. Thus, for example, if RF signal information, occupying e.g., the 4-6 GHz band, is modulated onto the outer branch of the slave laser path, one would be able to demodulate it with just a photodiode onto an IF equal to the chosen offset, e.g., at 12 GHz, some number of kilometers away from a coupled optical fiber.

Figure 9 shows a third example of the use of an OPLL for frequency synthesis [57]. Here, an external stable microresonator is used as the reference source, and an SGDBR-PIC and OPLL circuit similar to that in Fig. 7 is employed to select and lock to a microresonator line, providing a high-level stable output at the precise frequency of the reference resonator plus the tunable RF offset. What is particularly interesting is that the SGDBR can tune to a given line, lock to it, and provide a stable output within 200 ns, as shown by the repetitive switching back and forth between two SGDBR laser open loop frequencies some 5.72 nm or 720 GHz apart. The RF synthesizer is tuned to provide the difference necessary to get within locking range, here 2.5 GHz. The microresonator mode spacing in this wavelength range is ∼25.7 GHz, suggesting that the SGDBR laser is jumping across 28 resonator modes to relock in this experiment. The mode spacing varies slightly due to dispersion.

### B. High Power InP SoC-PICs for Free-Space Optical Links

The high data rates and low cost, size, weight and power (CSWaP) offered by SoC-PICs makes them desirable for free space laser communications to provide connectivity for intersatellite and deep-space links [58]. Figure 10(a) illustrates an InP-based PIC transmitter for free space optical communications [59]. The transmitter consists of a SGDBR
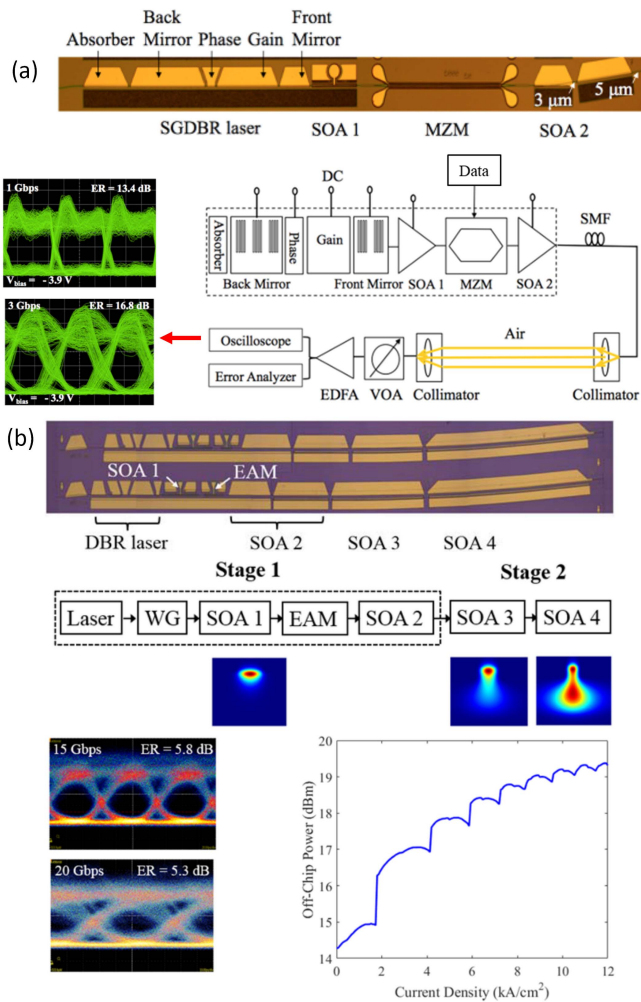
Fig. 10. Free-space link experiments. (a) SoC-PIC photo, schematic and data from free-space link experiment. Adapted with permission from [59]; (b) demonstration of high-power PIC with expanded mode SOA, and output power up to 19 dBm and 20 Gb/s data rate. Adapted with permission from [60].



Fig. 11. $CO_2$ sensor SoC-PIC photo, schematic/electronics, and results. The first laser (leader) is frequency locked to a reference $CO_2$ cell, and a second laser (follower) is successively offset phase locked to the leader to trace out the $CO_2$ gas absorption in the atmosphere within a LIDAR path. Adapted with permission from [61].

laser, high-speed SOA, MZM, and a high-power output booster SOA. The SGDBR laser tunes from 1521 to 1565 nm with >45 dB side mode suppression ratio (SMSR). This InP PIC was incorporated into a free space optical link to demonstrate the potential for low size, weight and power demonstrating its suitability for deployment on small aircraft or satellites. Error-free operation was achieved at 3 Gbps for an equivalent link length of 180 m (up to 300 m with forward error correction) with a maximum output power of 14.5 dBm (28 mW).

A modified transmitter design for higher power operation is shown in Fig. 10(b) [60]. This PIC uses a quantum well intermixing (QWI) platform, rather than offset quantum well (OQW), for active-passive integration. The QWI transmitter consists of a DBR laser, high-speed SOA, an EAM, and an output SOA. The epitaxial structure and waveguide were modified in this design to achieve a lower confinement factor in the SOA for higher output saturation power. The measured off-chip power is 19.5 dBm (90 mW), and a data rate of 20 Gbps was demonstrated.
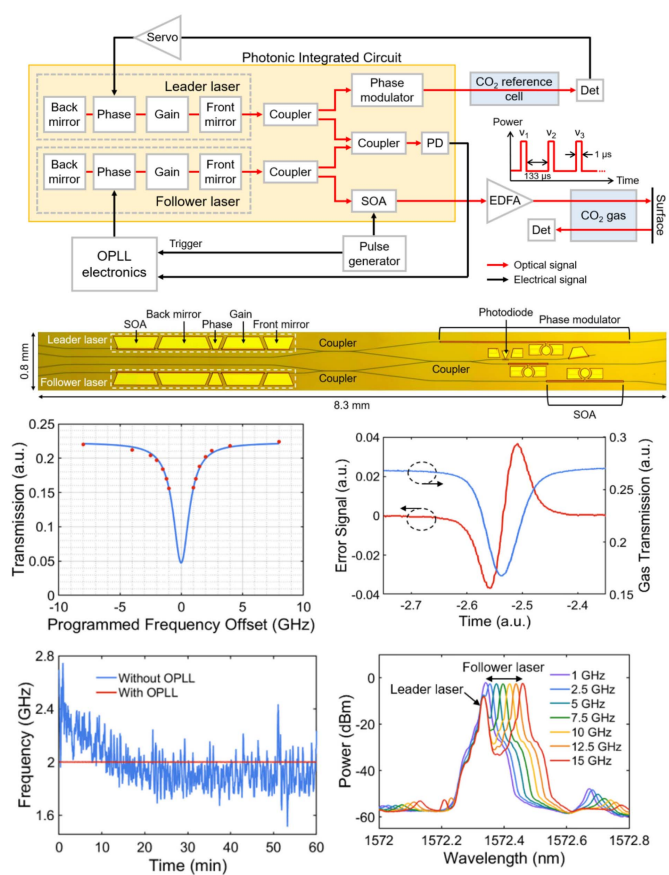
### C. Remote Gas Sensing LIDAR

SoC-PICs for LIDAR have also been demonstrated recently at UCSB for gas sensing applications. The system shown in Figure 11 is for detection of atmospheric carbon dioxide ($CO_2$) using integrated path differential absorption LIDAR as described in [61]. Again, this system takes advantage of the low CSWaP offered by SoC-PICs to make it suitable for deployment on satellites. The InP PIC contains two SGDBR lasers, a leader and follower. The leader laser is locked to the center of the 1572.335 nm $CO_2$ absorption line, using the $CO_2$ reference cell as shown in the upper part of the system diagram. The frequency stability of the leader laser is improved 236-fold when locked to the gas cell, compared to free-running. The follower laser is tuned ±15 GHz around the 1572.335 nm absorption line and offset locked to the leader with an OPLL. The SOA is used to generate pulses at each frequency step to sample the $CO_2$ absorption line.

### D. Widely Tunable 1030 nm SGDBR Laser PIC

The widely-tunable SoC-PICs discussed so far have all been demonstrated on InP and as such are restricted to wavelengths in the 1300-1600 nm range. Further development is being pursued, however, to develop widely-tunable PICs for
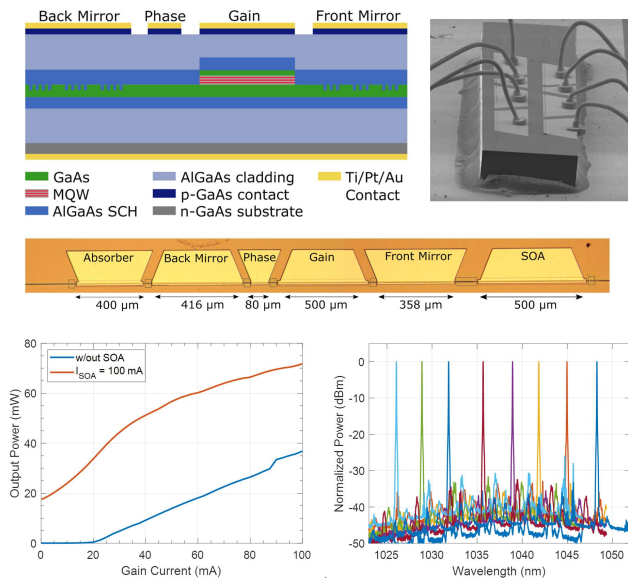
Fig. 12. Widely tunable SGDBR laser on GaAs, demonstrating 22 nm of continuous tuning around 1030 nm and up to 75 mW output power with amplification. For more information see [64] and [65].

applications in other spectral regions. Here, recent work on the development of widely-tunable SGDBR lasers on gallium arsenide (GaAs) for 1030 nm LIDAR is demonstrated. The spectral region near 1 $\mu$m is of particular interest for airborne terrain mapping LIDAR systems [62], owing to relatively low atmospheric absorption and the existence of high-quality detectors at this wavelength [63]. As with the remote gas sensing LIDAR system discussed above, the reduction of CSWaP offered by a SoC-PIC, compared to a system with commercial off-the-shelf (CoTS) components, is of critical importance for airborne topographical LIDAR.

A widely tunable SGDBR laser and integrated SOA on GaAs with a center wavelength near 1030 nm has been fabricated at UCSB and is shown in Fig. 12. This device was fabricated on an OQW PIC platform for active-passive integration, adapted for the GaAs material system [64]. The standalone SGDBR laser demonstrates 22.3 nm of continuous wavelength tuning with 30 dB SMSR (bottom right of Fig. 12) and 35 mW of output power [65]. With the addition of an integrated SOA, the output power can be increased to greater than 75 mW (bottom left of Fig. 12). The demonstration of a widely tunable laser and integrated SOA on GaAs lays a path for further development of more complex SoC-PICs in the 1 $\mu$m spectral range, analogous to those on InP for C-band applications.

## V. Conclusion

Advanced materials growth and processing technologies together with highly-developed device designs have enabled complex PICs on III-Vs that can perform several photonic system functions. Many of these SoC-PICs can provide significant savings in cost, size, weight, and power compared to discrete implementations, even eliminating the need for some components, or required electronics, in many cases.

In this paper we have focused on the development, and benefits of widely-tunable lasers in such SoC-PICs. The use of such lasers can provide wavelength agility for broadband WDM communication systems, wavelength stability by phase locking to any of a number of references, and wavelength sweeping for a variety of sensing applications, such as in LIDAR or optical beam control.

### References

[1] F. Kish et al., "System-on-chip photonic integrated circuits," IEEE J. Sel. Topics Quantum Electron., vol. 24, no. 1, pp. 1–20, Feb. 2018.

[2] K. A. Williaams et al., "InP photonic circuits using generic integration," Photon. Res., vol. 3, no. 5, pp. 60–67, 2015.

[3] Y. Tohmori, Y. Suematsu, H. Tsushima, and S. Arai, "Wavelength tuning of GaInAsP/InP integrated laser with butt-jointed built-in distributed Bragg reflector," Electron. Lett., vol. 19, no. 17, pp. 656–657, 1983.

[4] M. Zirngibl, C. H. Joyner, and L. W. Stulz, "WDM receiver by monolithic integration of an optical preamplifier, waveguide grating router and photodiode array," Electron. Lett., vol. 31, no. 7, pp. 581–582, 1995.

[5] K. Kudo et al., "1.55-$\mu$m wavelength-selectable microarray DFB-LD's with monolithically integrated MMI combiner, SOA, and EA-modulator," IEEE Photon. Technol. Lett., vol. 12, no. 3, pp. 242–244, Mar. 2000.

[6] M. C. Larson et al., "Narrow linewidth sampled-grating distributed Bragg reflector laser with enhanced side-mode suppression," in Conf. Opt. Fiber Commun. Tech. Dig. Ser., Jun. 2015, pp. 2–4.

[7] G. Gilardi and M. K. Smit, "Generic InP-based integration technology: Present and prospects (invited review)," Prog. Electromagn. Res., vol. 147, pp. 23–35, 2014.

[8] L. A. Coldren et al., "High performance InP-based photonic ICs—A tutorial," J. Lightw. Technol., vol. 29, no. 4, pp. 554–570, Feb. 15, 2011.

[9] M. Smit, K. Williams, and J. van der Tol, "Past, present, and future of InP-based photonic integration," APL Photon., vol. 4, no. 5, May 2019, Art. no. 050901, doi: 10.1063/1.5087862.

[10] G. E. Hoefler et al., "Foundry development of system-on-chip InP-based photonic integrated circuits," IEEE J. Sel. Topics Quantum Electron., vol. 25, no. 5, pp. 1–17, Sep. 2019.

[11] M. Blaicher et al., "Hybrid multi-chip assembly of optical communication engines by in situ 3D nano-lithography," Light, Sci. Appl., vol. 9, no. 1, pp. 1–11, Dec. 2020, doi: 10.1038/s41377-020-0272-5.

[12] J. Zhang et al., "III-V-on-Si photonic integrated circuits realized using micro-transfer-printing," APL Photon., vol. 4, no. 11, Nov. 2019, Art. no. 110803, doi: 10.1063/1.5120004.

[13] B. Song, C. Stagarescu, S. Ristic, A. Behfar, and J. Klamkin, "3D integrated hybrid silicon laser," Opt. Exp., vol. 24, no. 10, pp. 10435–10444, 2016.

[14] Y. Wan et al., "Low threshold quantum dot lasers directly grown on unpatterned quasi-nominal (001) Si," IEEE J. Sel. Topics Quantum Electron., vol. 26, no. 2, pp. 1–9, Mar. 2020.

[15] C. Xiang et al., "High-performance silicon photonics using heterogeneous integration," IEEE J. Sel. Topics Quantum Electron., vol. 28, no. 3, pp. 1–15, May 2022.

[16] N. Margalit, C. Xiang, S. M. Bowers, A. Bjorlin, R. Blum, and J. E. Bowers, "Perspective on the future of silicon photonics and electronics," *Appl. Phys. Lett.*, vol. 118, no. 22, May 2021, Art. no. 220501.

[17] S. E. Miller, "Integrated optics: An introduction," *Bell Syst. Tech. J.*, vol. 48, no. 7, pp. 2059–2069, Sep. 1969.

[18] D. B. Keck, R. D. Maurer, and P. C. Schultz, "On the ultimate lower limit of attenuation in glass optical waveguides," *Appl. Phys. Lett.*, vol. 22, no. 7, pp. 307–309, Apr. 1973.

[19] T. L. Koch *et al.*, "GaInAs/GaInAsP multiple-quantum-well integrated heterodyne receiver," *Electron. Lett.*, vol. 25, no. 24, pp. 1621–1623, 1989.

[20] R. C. Alferness and A. Glass, "Bell labs technology trends & developments," *Bell Labs Tech. J.*, vol. 2, no. 2, pp. 1–15, 1988.

[21] K. Murata, S. Mito, and I. Kobayashi, "Over 720 GHz (5.8 nm) frequency tuning by a 1.5 $\mu$m DBR laser with phase and Bragg wavelength control regions," *Electron. Lett.*, vol. 23, no. 8, pp. 403–405, 1987.

[22] T. L. Koch, U. Koren, and B. I. Miller, "High performance tunable 1.5 $\mu$m InGaAs/InGaAsP multiple quantum well distributed Bragg reflector lasers," *Appl. Phys. Lett.*, vol. 53, no. 12, pp. 1036–1038, 1988.

[23] R. J. Mears, L. Reekie, I. M. Jauncey, and D. N. Payne, "Low-noise erbium-doped fibre amplifier operating at 1.54 $\mu$m," *Electron. Lett.*, vol. 23, no. 19, pp. 1026–1028, 1987.

[24] L. A. Coldren, B. I. Miller, K. Iga, and J. A. Rentschler, "Monolithic two-section GaInAsP/InP active-optical-resonator devices formed by reactive ion etching," *Appl. Phys. Lett.*, vol. 38, no. 5, pp. 315–317, Mar. 1981.

[25] L. A. Coldren, "Multi-section tunable laser with differing multi-element mirrors," U.S. Patent 4 896 325, Jan. 23, 1990.

[26] V. Jayaraman, Z.-M. Chuang, and L. A. Coldren, "Theory, design, and performance of extended tuning range semiconductor lasers with sampled gratings," *IEEE J. Quantum Electron.*, vol. 29, no. 6, pp. 1824–1834, Jun. 1993.

[27] V. Jayaraman, A. Mathur, L. A. Coldren, and P. D. Dapkus, "Very wide tuning range in a sampled grating DBR laser," in *Proc. 13th IEEE Int. Semiconductor Laser Conf.* Takamatsu, Japan, 1992, Paper PD-11.

[28] T. L. Koch, "OFC tutorial: III–V and silicon photonic integrated circuit technologies," in *Proc. OFC/NFOEC*, 2012, pp. 1–45.

[29] Y. A. Akulova *et al.*, "Widely tunable electroabsorption-modulated sampled-grating DBR laser transmitter," *IEEE J. Sel. Top. Quantum Electron.*, vol. 8, no. 6, pp. 1349–1357, Nov./Dec. 2002.

[30] Y. A. Akulova *et al.*, "10 Gb/s Mach–Zehnder modulator integrated with widely-tunable sampled grating DBR laser," in *Proc. OSA Trends Opt. Photon. Ser.*, vol. 95, 2004, pp. 395–397.

[31] C. Coldren *et al.*, "Reliability of widely-tunable SGDBR lasers suitable for deployment in agile networks," in *OFC Tech. Dig.*, vol. 1, 2003, pp. 73–75.

[32] *Tunable Multiprotocal XFP Optical Transceiver—1550 nm for up to 80 km Reach JXP Series, P/N JXP01TMAC1CX5*, Lumentum, San Jose, CA, USA, 2015.

[33] Lumentum Operations LLC. (Mar. 2018).*Lumentum to acquire OCLARO for 1.8B in cash and stock*. San Jose, CA, Accessed: Apr. 26, 2022. [Online]. Available: https://www.lumentum.com/en/media-room/news-releases/lumentum-acquire-oclaro-18b-cash-and-stock

[34] R. C. Alferness *et al.*, "Broadly tunable InGaAsP/InP laser based on a vertical coupler filter with 57-nm tuning range," *Appl. Phys. Lett.*, vol. 60, no. 26, pp. 3209–3211, 1992.

[35] M. Öberg, S. Nilsson, K. Streubel, J. Wallin, L. Bäckbom, and T. Klinga, "74 nm wavelength tuning range of an InGaAsP/InP vertical grating assisted codirectional coupler laser with rear sampled grating reflector," *IEEE Photon. Technol. Lett.*, vol. 5, no. 7, pp. 735–738, Jul. 1993.

[36] L. A. Coldren, "Monolithic tunable diode lasers," *IEEE J. Sel. Topics Quantum Electron.*, vol. 6, no. 6, pp. 988–999, Nov./Dec. 2000.

[37] R.-J. Essiambre, G. Kramer, P. J. Winzer, G. J. Foschini, and B. Goebel, "Capacity limits of optical fiber networks," *J. Lightw. Technol.*, vol. 28, no. 4, pp. 662–701, Feb. 15, 2010.

[38] M. G. Young *et al.*, "Six wavelength laser array with integrated amplifier and modulator," *Electron. Lett.*, vol. 31, no. 21, pp. 1835–1836, Oct. 1995.

[39] H. M. Hatakeyama *et al.*, "Wavelength-selectable microarray light sources for S-, C-, and L-band WDM systems," *IEEE Photon. Technol. Lett.*, vol. 15, no. 7, pp. 903–905, Jul. 2003.

[40] N. Kikuchi *et al.*, "Monolithically integrated 64-channel WDM wavelength-selective receiver," *Electron. Lett.*, vol. 39, no. 3, pp. 312–314, 2003.

[41] J. Heanue, E. Vail, M. Sherback, and B. Pezeshki, "Widely tunable laser module using DFB array and MEMs selection with internal wavelength locker," in *Proc. OFC*, vol. 1, 2003, pp. 21–22.

[42] M. Smit *et al.*, "A generic foundry model for InP-based photonic ICs," in *Proc. Opt. InfoBase Conf. Paper*, 2012, pp. 2–4.

[43] R. Nagarajan *et al.*, "Large-scale photonic integrated circuits," *IEEE J. Sel. Top. Quantum Electron.*, vol. 11, no. 1, pp. 50–65, Jan./Feb. 2005.

[44] M. M. Dummer, J. Klamkin, A. Tauke-Pedretti, and L. A. Coldren, "A bit-rate-transparent monolithically integrated wavelength converter," in *Proc. Eur. Conf. Opt. Commun. (ECOC)*, vol. 4, Sep. 2008, pp. 77–80.

[45] S. C. Nicholes, M. L. Mašanović, B. Jevremović, E. Lively, L. A. Coldren, and D. J. Blumenthal, "An $8 \times 8$ InP monolithic tunable optical router (MOTOR) packet forwarding chip," *J. Lightw. Technol.*, vol. 28, no. 4, pp. 641–650, Feb. 15, 2010.

[46] M. Lu *et al.*, "An integrated 40 Gbit/s optical Costas receiver," *J. Lightw. Technol.*, vol. 31, no. 13, pp. 2244–2253, Jul. 1, 2013.

[47] H. C. Park *et al.*, "40 Gbit/s coherent optical receiver using a Costas loop," *Opt. Exp.*, vol. 20, no. 26, pp. 197–203, 2012.

[48] W. Guo, P. R. A. Binetti, M. L. Masanovic, L. A. Johansson, and L. A. Coldren, "Large-scale InP photonic integrated circuit packaged with ball grid array for 2D optical beam steering," in *Proc. IEEE Photon. Conf. (IPC)*, Sep. 2013, pp. 651–652.

[49] M. Lauermann *et al.*, "Multi-channel, widely-tunable coherent transmitter and receiver PICs operating at 88 Gbaud/16-QAM," in *Proc. Opt. Fiber Commun. Conf. Exhib. (OFC)*, vol. 1, 2017, pp. 8–10.

[50] A. Tauke-Pedretti *et al.*, "Separate absorption and modulation Mach–Zehnder wavelength converter," *J. Lightw. Technol.*, vol. 26, no. 1, pp. 91–98, Jan. 1, 2008.

[51] V. Lal, M. L. Mašanović, J. A. Summers, G. Fish, and D. J. Blumenthal, "Monolithic wavelength converters for high-speed packet-switched optical networks," *IEEE J. Sel. Top. Quantum Electron.*, vol. 13, no. 1, pp. 49–57, Jan./Feb. 2007.

[52] W. Guo *et al.*, "Two-dimensional optical beam steering with InP-based photonic integrated circuits," *IEEE J. Sel. Topics Quantum Electron.*, vol. 19, no. 4, Jul. 2013, Art. no. 6100212.

[53] M. Lu *et al.*, "A highly integrated optical phase-locked loop with singlesideband frequency sweeping," *CLEO Sci. Innov.*, vol. 20, no. 9, pp. 1090–1092, 2012.

[54] S. Ristic, A. Bhardwaj, M. J. Rodwell, L. A. Coldren, and L. A. Johansson, "An optical phase-locked loop photonic integrated circuit," *J. Lightw. Technol.*, vol. 28, no. 4, pp. 526–538, Feb. 15, 2010.

[55] A. Simsek *et al.*, "Evolution of chip-scale heterodyne optical phase-locked loops toward Watt level power consumption," *J. Lightw. Technol.*, vol. 36, no. 2, pp. 258–264, Jan. 15, 2018.

[56] S. Arafin, A. Simsek, M. Lu, M. J. Rodwell, and L. A. Coldren, "Heterodyne locking of a fully integrated optical phase-locked loop with on-chip modulators," *Opt. Lett.*, vol. 42, no. 19, pp. 3745–3748, 2017.

[57] S. Arafin *et al.*, "Towards chip-scale optical frequency synthesis based on optical heterodyne phase-locked loop," *Opt. Exp.*, vol. 25, no. 2, pp. 681–694, 2017.

[58] H. Hemmati, A. Biswas, and I. B. Djordjevic, "Deep-space optical communications: Future perspectives and applications," *Proc. IEEE*, vol. 99, no. 11, pp. 2020–2039, Nov. 2011.

[59] H. Zhao *et al.*, "Indium phosphide photonic integrated circuits for free space optical links," *IEEE J. Sel. Topics Quantum Electron.*, vol. 24, no. 6, pp. 1–6, Nov. 2018.

[60] H. Zhao *et al.*, "High-power indium phosphide photonic integrated circuits," *IEEE J. Sel. Topics Quantum Electron.*, vol. 25, no. 6, pp. 1–10, Nov. 2019.

[61] J. Fridlander *et al.*, "Dual laser indium phosphide photonic integrated circuit for integrated path differential absorption LiDAR," *IEEE J. Sel. Topics Quantum Electron.*, vol. 28, no. 1, pp. 1–8, Jan. 2022.

[62] A. W. Yu *et al.*, "A 16-beam non-scanning swath mapping laser altimeter instrument," *Proc. SPIE*, vol. 8599, Mar. 2013, Art. no. 85990P.

[63] M. A. Krainak, X. Sun, G. Yang, and W. Lu, "Comparison of linear-mode avalanche photodiode LiDAR receivers for use at one-micron wavelength," *Proc. SPIE*, vol. 7681, Apr. 2010, Art. no. 76810Y.

[64] P. Verrinder *et al.*, "Gallium arsenide photonic integrated circuit platform for tunable laser applications," *IEEE J. Sel. Topics Quantum Electron.*, vol. 28, no. 1, pp. 1–9, Jan. 2022.

[65] P. Verrinder, L. Wang, F. Sang, V. Rosborough, M. Nickerson, G. Yang, et al., "SGDBR tunable laser on gallium arsenide for 1030 nm lidar applications," in*Proc. 27th Int. Semiconductor Laser Conf.* Potsdam, Germany, Oct. 10/14, 2021, Paper no. WA2.2.

**Larry A. Coldren** (Life Fellow, IEEE) received the B.S. degree in electrical engineering and the B.A. degree in physics from Bucknell University and the M.S. and Ph.D. degrees in electrical engineering from Stanford University in 1969 and 1972, respectively, under the support of Bell Laboratories.

He joined Bell Laboratories in 1968. Following 13 years in the research area with Bell Laboratories, he joined the ECE Department of the University of California at Santa Barbara (UCSB) in 1984. In 1986, he was a Founding Member of the Materials Department. He became the Fred Kavli Professor of optoelectronics and sensors in 1999. From 2009 to 2011, he was the Acting Dean of the College of Engineering, and in 2017, he became a Emeritus Professor and a Distinguished Research Professor. In 1990, he co-founded Optical Concepts, later acquired as Gore Photonics, to develop novel VCSEL technology, and in 1998, he co-founded Agility Communications, later acquired by JDSU (now Lumentum), to develop widely-tunable integrated transmitters and transponders. At UCSB, he has worked on multiple-section widely-tunable lasers and efficient vertical-cavity surface-emitting lasers (VCSELs). He continues to research high-performance InP-based photonic integrated circuits, and high-speed and high-efficiency VCSELs for various applications. He has authored or coauthored over 1000 journals and conference papers, eight book chapters, a widely-used textbook, and 63 issued patents.

Prof. Coldren is a fellow of OSA, IEE, and the National Academy of Inventors as well as a member of the National Academy of Engineering. He was a recipient of the 2004 John Tyndall, the 2009 Aron Kressel, the 2014 David Sarnoff, the 2015 IPRM, and the 2017 Nick Holonyak, Jr., Awards.

**Jonathan Klamkin** (Senior Member, IEEE) received the B.S. degree from Cornell University, Ithaca, NY, USA, and the M.S. and Ph.D. degrees from the University of California at Santa Barbara (UCSB), Santa Barbara, CA, USA. From 2008 to 2011, he was a member of the Technical Staff with the Electro-Optical Materials and Devices Group, MIT Lincoln Laboratory, Lexington, MA, USA. From 2011 to 2013, he was an Assistant Professor with the Institute of Communication, Information and Perception Technologies, Scuola Superiore Sant'Anna, Pisa, Italy. From 2013 to 2015, he was an Assistant Professor of electrical and computer engineering (ECE) and materials with Boston University, Boston, MA. In 2015, he joined the ECE Department, University of California at Santa Barbara, where he is currently a Professor and the Director of the UCSB Nanotech. He has authored or coauthored 200 journals and conference papers. He or his group members were the recipient of Best Paper Awards at the 2006 Conference on Optoelectronic and Microelectronic Materials and Devices, the 2007 Microwave Photonics Conference, and the 2017 and 2019 Asia Communications and Photonics Conference. He was the recipient of the NASA Early Career Faculty Award, the DARPA Young Faculty Award, and the DARPA Director's Fellowship.

**Paul A. Verrinder** received the B.S. degree in electrical engineering from California State University, Fresno, in 2015, and the M.S. degree in electrical and computer engineering from the University of California at Santa Barbara (UCSB), Santa Barbara, in 2020, where he is currently pursuing the Ph.D. degree with the Electrical and Computer Engineering Department. From 2015 to 2018, he was an Electrical Engineer with NAVAIR, China Lake. His research interests are in integrated photonics for optical communications and LIDAR.